

DOI: 10.1002/cplu.201300343

 **Synthesis of Hybrid Cyclic Peptoids and Identification of Autophagy Enhancer**Kolla Rajasekhar,^[a] Nagarjun Narayanaswamy,^[a] Piyush Mishra,^[b] S. N. Suresh,^[b]
Ravi Manjithaya,^[b] and T. Govindaraju*^[a]

Cyclic peptoids are potential candidates for diverse biological activities. However, applications of cyclic peptoids are limited by the synthetic difficulties, conformational flexibility of large cyclic peptoids, and lack of secondary amide in the backbone. Herein, an elegant methodology for the synthesis of small and medium-size cyclic hybrid peptoids is developed. ¹⁵N-Alkyl and ¹⁵N-acyl substituents in *N*-(2-aminoethyl)glycine monomers enforce intra- and intermolecular cyclization to form stable six- and 12-membered cyclic products, respectively. NMR studies show inter- and intramolecular hydrogen bonding in six- and 12-membered cyclic peptoids, respectively. Screening of a cyclic peptoid library resulted in the identification of a potential candidate that enhanced autophagic degradation of cargo in a live cell model. Such upregulation of autophagy using small molecules is a promising approach for elimination of intracellular pathogens and neurodegenerative protein aggregates.

Peptides have emerged as promising therapeutic agents in recent years owing to their inexpensive synthesis, efficacy, specificity, and low toxicity. However, high susceptibility to proteolysis, flexibility, short half-life, denaturation, and poor target delivery and bioavailability make peptides practically less viable candidates for therapeutics. The deficiencies of linear peptides can be addressed by macrocyclization and crosslinking, which provide proper conformational stability.^[1] Although cyclic peptides offer relative stability and cell penetration efficiency, they also suffer from low *in vivo* stability and bioavailability. To address the inherent drawbacks of natural peptides, promising peptidomimetics have been developed.^[2] In particular peptoids, oligomers of *N*-substituted glycine with distinct

unnatural structure, possess numerous advantages. Peptoids have long half-lives owing to proteolytic resistance and good cell permeability resulting in greater bioavailability.^[3] However, major limitations of peptoids are their conformational flexibility and lack of secondary interactions, which can reduce the selectivity and sensitivity. Yet again, the macrocyclization of peptoids has been pursued to restrict conformational flexibility.^[4] Applications of cyclic peptoids are limited by the synthetic procedures and lack of secondary amide in the backbone. The most challenging aspect of cyclic peptidomimetics synthesis is the ring-closure event.^[5] The yields obtained in cyclization of longer oligomers are very moderate and the cyclization of short oligomers suffers from poor yields.^[1] An increase in ring size of cyclic peptidomimetics reduces bioactivity as a result of enhanced flexibility. This reiterates the importance of small/medium-size cyclic peptoids.

The linear and cyclic peptidomimetics have been studied for antimicrobial activity, DNA interaction, and autophagy modulation.^[6] Autophagy is a key mechanism for long-lived protein degradation and organelle turnover, and serves as a critical adaptive response that recycles energy and nutrients during starvation or stress. Small molecules have been utilized as probes to understand mechanisms as well as the relationship between autophagy and disease.^[7]

Herein, we report coupling-reagent-free differential cyclization of *N*-(2-aminoethyl)glycine (*aeg*) hybrid peptoid monomer into six- and 12-membered cyclic peptoids. In the literature, *aeg* has been used extensively as a backbone unit for the synthesis of peptide nucleic acids.^[8] Our choice of *aeg* monomer stemmed from the fact that among other advantages, small and medium-size hybrid cyclic peptoids are formed with secondary amide bonds and stable conformation. Further, we employed a simple design strategy wherein ¹⁵N-alkyl substituents keep the flexibility intact, whereas ¹⁵N-acyl substituents introduce rigidity and restricted bond rotation in the *aeg* backbone. Thus, *aeg* monomers with distinct ¹⁵N substituents and conformational features are expected to follow different modes of cyclization. To the best of our knowledge, this is the first report wherein *aeg* monomer has been used for direct synthesis of six- and 12-membered hybrid cyclic peptoids under coupling-reagent-free conditions. This cyclic peptoid library was screened to identify modulators of the autophagy process.

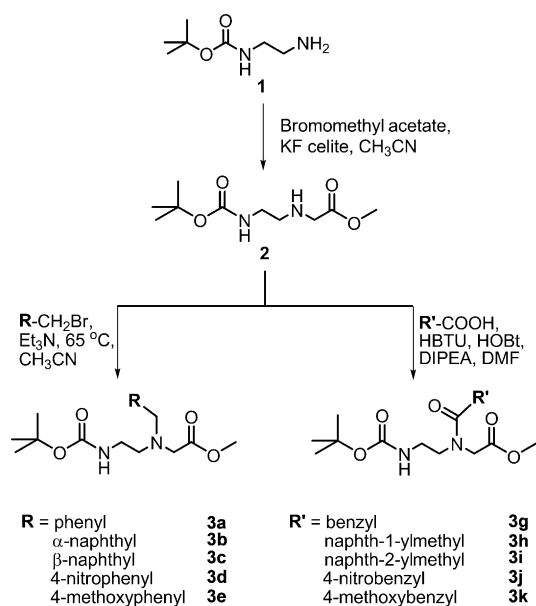
The *aeg* backbone was synthesized from mono *tert*-butoxycarbonyl (Boc)-protected ethylenediamine **1** (Scheme 1). The amine **1** was subjected to controlled mono-¹⁵N-alkylation by treatment with bromomethyl acetate using KF celite to obtain Boc-protected *aeg* methyl ester **2**. Then, the second ¹⁵N-alkyla-

[a] K. Rajasekhar, N. Narayanaswamy, Dr. T. Govindaraju
Bioorganic Chemistry Laboratory
New Chemistry Unit
Jawaharlal Nehru Centre for Advanced Scientific Research
Jakkur P.O., Bangalore 560064 (India)
Fax: (+91) 80-2208-2627
E-mail: tgraju@jncasr.ac.in
Homepage: <http://www.jncasr.ac.in/tgraju/>

[b] P. Mishra, S. N. Suresh, Dr. R. Manjithaya
Molecular Biology and Genetics Unit
Jawaharlal Nehru Centre for Advanced Scientific Research
Jakkur P.O., Bangalore 560064 (India)

 Supporting information for this article is available on the WWW under <http://dx.doi.org/10.1002/cplu.201300343>.

 This article is part of the "Early Career Series". To view the complete series, visit: <http://chempluschem.org/earlycareer>.



Scheme 1. Synthesis of Boc-protected α -N-alkyl (**3a–e**) and α -N-acyl (**3g–k**) modified *aeg* methyl ester monomers. HBTU = 2-(1*H*-benzotriazole-1-yl)-1,1,3,3-tetramethyluronium hexafluorophosphate, HOBT = *N*-hydroxybenzotriazole, DIPEA = *N,N*-diisopropylethylamine, DMF = *N,N*-dimethylformamide.

tion of amine **2** was performed with bromomethyl derivatives using triethylamine as base to obtain excellent yields of methyl esters of Boc-protected α -N-alkyl-*aeg* monomers **3a–e** (Scheme 1). The amine **2** was coupled to acetic acid derivatives to yield methyl esters of Boc-protected α -N-acyl-*aeg* monomers **3g–k**. The Boc-protected α -N-benzyl-*aeg* methyl ester monomer (**3a**) was subjected to in situ Boc deprotection and subsequent cyclization at 110 °C in *sec*-butanol containing 1% acetic acid (Table 1).^[9] The monomer **3a** underwent intramolecular cyclization to form six-membered cyclic product **4a**. Interestingly, under similar conditions α -N-(2'-phenylacetyl)-*aeg* methyl ester (**3g**) gave a very good yield of 12-membered hybrid cyclic peptoid **4g** through intermolecular cyclization (Table 2). To ascertain the generality of this differential cyclization, we tested variable functionalities for α -N-alkyl and α -N-acyl substituents (Tables 1 and 2). All the monomers were subjected to in situ Boc deprotection and subsequent cyclization. The peptoid monomers with α - and β -naphthalene functionalities (α -N-alkyl: **3b**, **3c** and α -N-acyl: **3h**, **3i**, respectively) were chosen to demonstrate if ring cyclization is independent of the type of aromatic moiety and position of attachment. Monomers having electron-withdrawing (4-nitrophenyl, **3d** and **3j**) and -donating (4-methoxyphenyl, **3e** and **3k**) groups were selected to study the influence of electronic effects on cyclization. Interestingly, the propensity of differential cyclization was found to be general, as the α -N-alkyl- and α -N-acyl-substituted *aeg* monomers formed six- and 12-membered products (**4b–e** and **4h–k**), respectively. The monomer **3f** with ethyl linker in the α -N-alkyl substituent also gave six-membered product **4f** (Table 1). This further confirmed our assumption that the flexibility of α -N-alkyl-*aeg* favors intramolecular cyclization. In contrast, the carbonyl group of the α -N-acyl substituent of *aeg* not only re-

Table 1. Intermolecular cyclization of α -N-alkyl-*aeg* monomers to six-membered cyclic products.

Reactant	Product	Yield [%] ^[a]
3a	4a	73
3b	4b	69
3c	4c	71
3d	4d	79
3e	4e	80
3f	4f	43

[a] Yields reported are of purified products.

stricted its free rotation but also rigidified the molecular conformation, thus favoring intermolecular cyclization to form 12-membered products. To extend the scope of this methodology, we synthesized adenine- and thymine-functionalized 12-membered products **4l** and **4m** (Table 2).

NMR and high-resolution mass spectroscopy (HRMS) product analysis confirmed the α -N-alkyl- and α -N-acyl-enforced differential cyclization of *aeg* methyl ester monomers. The ¹H NMR spectra (in labeled dimethyl sulfoxide, [D₆]DMSO) of monomer units (e.g., **3d** and **3j**) showed singlets at 1.5 and 3.7 ppm corresponding to Boc and methyl ester (–OCH₃) groups, respectively. In addition to the expected disappearance of the proton peak for the Boc group in the respective spectra of products (**4d** and **4j**), peaks for free amine (–NH₂) and –OCH₃ were absent, which indicates the possible cyclization of monomers (Figure 1 a). The ¹H NMR spectrum of product from **3d** showed four peaks (2', 3', 5', and 7') in the region 2.4–4.0 ppm, a broad peak at 7.85 ppm, and two doublets at 7.51–7.49 and 8.18–8.15 ppm corresponding to four –CH₂ amide protons (H_a) and four aromatic protons, respectively, which confirmed a six-membered cyclo-*aeg* structure for product **4d** (HRMS, mass =

Table 2. Intermolecular cyclization of α -N-alkyl-aeg monomers to 12-membered cyclic products.

Reactant	Product	Yield [%] ^[a]
3g	4g	72
3h	4h	68
3i	4i	76
3j	4j	82
3k	4k	68
3l	4l	78
3m	4m	72

[a] Yields reported are of purified products.

236.1055, $[M+H]^+$). The spectrum of product from **3j** (Figure 1a) showed a completely different splitting pattern including two amide peaks at 8.05 and 8.12 ppm for H_b and H_c , respectively, which indicated the possible product as either a trimer or a cyclic dimer. The trimer was ruled out by HRMS analysis (549.1664, $[M+Na]^+$), thus confirming the 12-membered cyclic dimer (*aeg-aeg*) product **4j**. Surprisingly, seven peaks in the region 3.0–4.3 ppm (2, 3, 5, 9, 11, 14, and 20) corresponding to protons of eight $-CH_2$ groups revealed that **4j** exists as a nonsymmetrical cyclic homodimer. The nonsymmetrical structure of **4j** was further established by ^{13}C NMR and

^{13}C DEPT-135 (distortionless enhancement by polarization transfer) studies (Figure S1 in the Supporting Information).

Next, we investigated the hydrogen-bonding patterns in representative examples **4d** and **4j** by temperature- and concentration-dependent studies.^[10] 1H NMR study revealed the presence of intermolecular hydrogen-bonding interactions in **4d** (Figure S2). For **4j**, 1H NMR spectra showed an upfield shift of 0.33 and 0.39 ppm, respectively, for the amide protons H_b and H_c with increasing temperature from 25 to 95 °C, thus confirming strong hydrogen-bonding interactions (Figure 1b). The nature of hydrogen bonding in **4j** was validated by a concentration-dependent NMR study. 1H NMR spectra with a decrease in concentration (dilution) of **4j** (3.8, 1.9, 0.95, 0.47, and 0.23 mM) did not show change in the peak position of H_a and H_c , which is possible only in the case of intramolecular hydrogen-bonding interactions (Figure S3). Such intramolecular hydrogen bonding can guide the structural conformation of cyclic peptidomimetics similar to that observed in cyclic peptides.^[11]

Temperature coefficient ($\Delta\delta_{NH}/\Delta T$) values^[12] of H_b and H_c were found to be -4.46 and -5.7 ppb, respectively. Therefore the strength of hydrogen bonding is moderate and amide protons are less shielded from the $[D_6]DMSO$. 1H NMR spectra of **4j** (Figure S4) in CD_3CN with increase in temperature showed an upfield shift of H_b and H_c (0.146 and 0.09 ppm) with temperature coefficient values -2.3 and -3.62 ppb, respectively (Figure S5). The higher values of the temperature coefficient suggest stronger hydrogen bonding and shielding of amide protons from the solvent (CD_3CN). Interestingly, the difference in upfield shifts of H_b and H_c and their corresponding temperature coefficient values suggest two hydrogen bonds with different bond length, which is evidence for a nonsymmetrical conformation of **4j**. Further, two sets of proton peaks of **4j** merge at higher temperature (>65 °C) to form one set, thereby demonstrating the transformation from nonsymmetrical to symmetrical conformation (Figure 1b).^[13] The 1H - ^{13}C HSQC spectrum obtained was remarkably well dispersed, indicative of a nonrepetitive folded conformation (Figure S6). The energy-minimized structure showed the *trans* conformation for amides, which allowed the conclusion that the molecule exists in a low-energy stable state (Figure 1c). The model structure also revealed two intramolecular hydrogen bonds between secondary amide protons and α -N-carbonyls (H_b and $C^{13}=O$ and H_c and $C^{19}=O$; Figure 1d). The two intramolecular hydrogen bonds in **4j** exhibit different bond lengths (1.96 and 2.01 Å for H_b and H_c , respectively), which supports the inference deduced from 1H NMR spectroscopy. The observed differential cyclization can be understood from the structural aspects of *aeg* monomers. The flexible α -N-alkyl-*aeg* methyl esters follow Baldwin rules of intramolecular cyclization (Figure S7).^[14] The terminal amine attacks the electrophilic methyl ester carbonyl group without

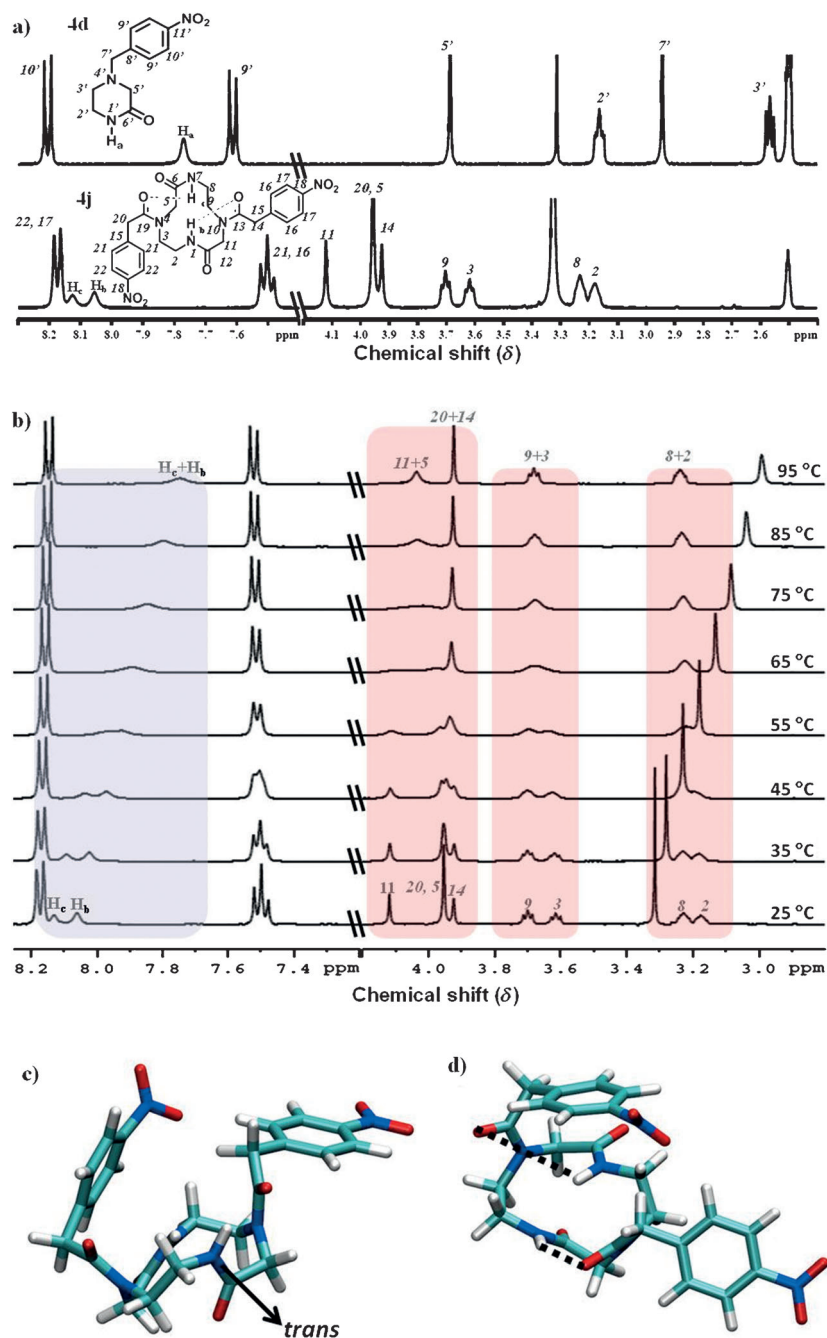


Figure 1. NMR studies and energy-minimized structure of **4j**. a) Comparative ¹H NMR spectra of cyclic products **4d** and **4j** ($[D_6]DMSO$). b) Variable-temperature ¹H NMR spectra of **4j** (in $[D_6]DMSO$). c, d) Energy-minimized model structure of **4j** showing *trans* amides and intramolecular hydrogen bonds (■■■■), respectively.

any hindrance to form six-membered products (**4a–e**), whereas in α -*N*-acyl-aeg methyl esters, conformational rigidity prevents the intramolecular reaction. Alternatively, intermolecular nucleophilic attack of the free amine of one monomer onto the methyl ester carbonyl group of another monomer is energetically favored to form 12-membered products (**4g–m**).

The cyclic peptoids being amphipathic in nature, we envisaged them to be permeable to biological cell membranes.^[15] We wanted to test if these peptoids are bioactive against cellular phenomena such as cell viability, and whether they would

affect specific cellular processes such as autophagy. Cyclic peptoids (**4a–m**) were tested for their ability to affect autophagy, a biological process involved in the turnover of proteins and organelles. The degradation of a cargo marker indicative of selective autophagy was followed over time in the yeast *Pichia pastoris* (Figure 2a). Interestingly, **4a** increased the rate of degradation of the protein marker through autophagy significantly in a dose-dependent manner (Figure 2b). Furthermore, the growth characteristics suggest **4a** is not toxic to yeast cells (Figure 2c–e). Microscopy studies in *Saccharomyces cerevisiae* showed a faster rate of peroxisome (green fluorescent protein (GFP)-labeled) degradation through autophagy in the presence of **4a** (50 μ M), as observed by the appearance of diffused GFP in the vacuole over time (arrowheads, Figure 2f,g). Strikingly, in the presence of **4a**, GFP appeared inside the vacuoles (Figure 2g, inset) at much earlier time points than for the untreated cells (Figure 2f, inset). To further confirm the activity of cyclic peptoid **4a**, GFP-autophagy-related protein 8 (GFP-Atg8) processing assay was performed. The cells were transferred to starvation conditions and free GFP released from GFP-Atg8 fusion protein was used as an indicator of autophagy flux. There were higher free GFP levels in cells treated with peptoid **4a**, which suggests an increase in autophagic flux (Figure 3). Thus, upregulation of autophagy by using

small molecules such as **4a** is a promising approach towards elimination of intracellular pathogens and neurodegenerative protein aggregates.^[7]

In summary, an elegant methodology for the synthesis of hybrid cyclic peptoids has been developed. The conformational flexibility and rigidity of the α -*N*-alkyl- and α -*N*-acyl-substituted *N*-(2-aminoethyl)glycine backbone enforce intra- and intermolecular cyclization, respectively, to form six- and 12-membered products. Unlike classical peptoids, our hybrid cyclic peptoids exhibit stable conformation and contain secondary amides

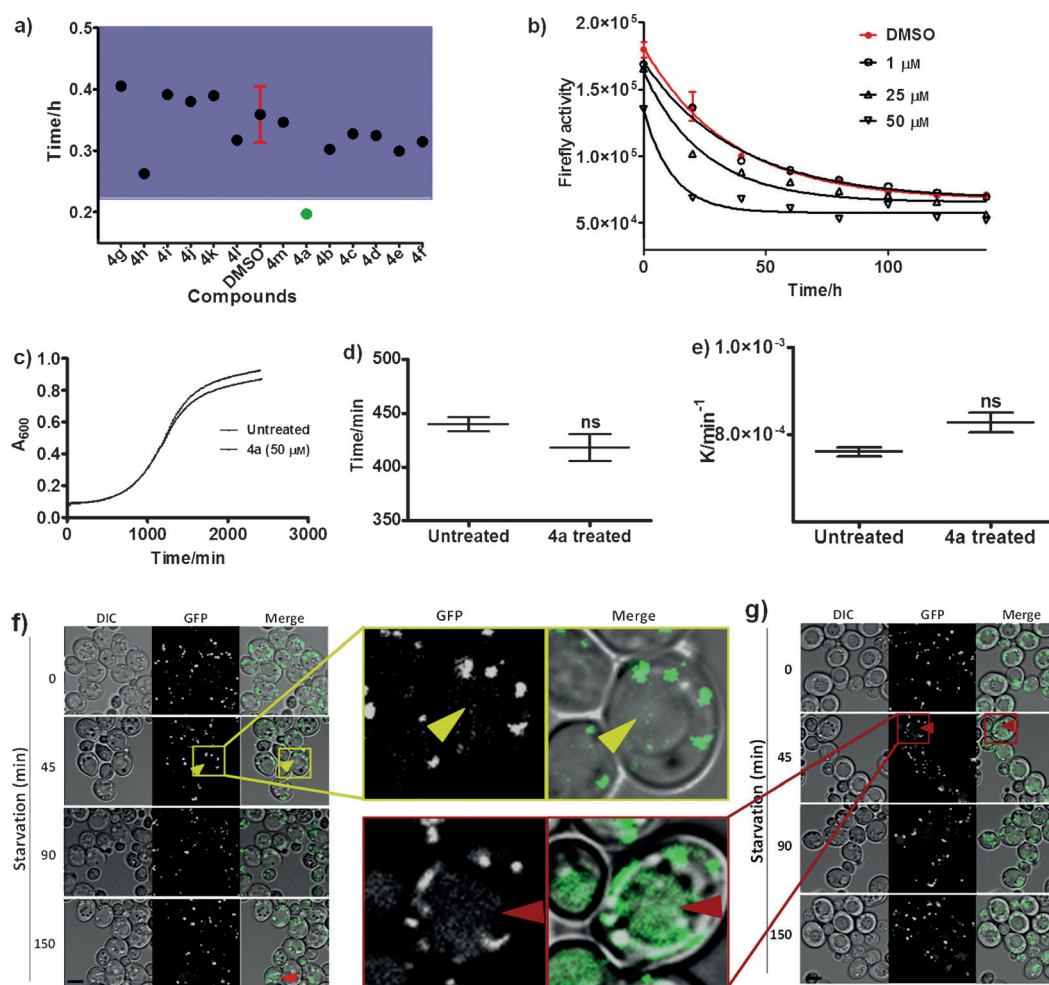


Figure 2. Autophagy studies in yeast. a) Time taken for a 50% decrease in cargo activity for the control (DMSO) and **4a–m** at 50 μM ; purple area denotes 3 standard deviation (SD) units. b) Dose response of **4a** (1, 25, and 50 μM) with time. Growth analysis of *Saccharomyces cerevisiae* in the presence and absence of **4a** was performed: c) growth curve, d) growth rate, e) doubling time were plotted using GraphPad Prism. f, g) Microscopy images showing degradation of peroxisomes (GFP) in the vacuole (arrowheads) in untreated (f) and **4a**-treated (g) cells. Scale bar: 4 μm . DIC = differential interference contrast, GFP = green fluorescent protein.

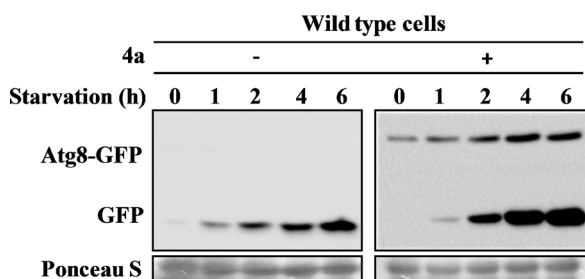


Figure 3. GFP-Atg8 processing assay. Peptoid **4a** increases GFP-Atg8 processing, as evident in later time points (at 4 and 6 h) relative to that of untreated cells. Atg8 = autophagy-related protein 8.

that may be useful for providing secondary interactions. Screening of a cyclic peptoids library gave an effective rate enhancer (**4a**) of autophagy. We are now working towards structure–activity relationships on **4a** as well as expanding our synthetic methodology to access the diverse hybrid cyclic peptoid library for numerous biological applications.

Experimental Section

General synthetic procedure for *N*-alkyl-^α*N*-(2-aminoethyl)-glycine methyl ester monomers

Triethylamine (2 mmol) was added to a solution of **2** (1.1 mmol) in acetonitrile (15 mL) at room temperature under an argon atmosphere and the mixture was stirred for 15 min. Then bromomethyl derivatives were added and the reaction mixture was heated at reflux (81 °C) for 6–8 h. The reaction was monitored by TLC, and on completion of reaction, the solvent was evaporated and the crude product was purified by silica gel column chromatography.

General synthetic procedure for ^α*N*-acyl-*N*-(2-aminoethyl)-glycine methyl ester monomers

2-(1*H*-Benzotriazole-1-yl)-1,1,3,3-tetramethyluronium hexafluorophosphate (HBTU, 1.2 mmol) was added to a solution of acetic acid derivatives (1 mmol) in DMF, followed by *N*-hydroxybenzotriazole (HOBT, 1.2 mmol) at ice-cooled temperature under an argon atmosphere. The reaction mixture was stirred until a clear solution was obtained, then compound **2** (1.1 mmol) followed by *N,N*-diisopro-

pylethylamine (DIPEA, 3 mmol) were added slowly in portions and the reaction mixture was stirred for 5–6 h at room temperature. The reaction was monitored by TLC, and on completion the reaction mixture was poured into water and extracted with CHCl_3 . The organic layer was dried over Na_2SO_4 , the solvent was evaporated, and the crude product was purified by silica gel column chromatography.

General synthetic procedure for cyclization

Trifluoroacetic acid (TFA) in dichloromethane (1:1, v/v; 5 mL) and a few drops of triisopropylsilane (TIPS) were added to a solution of Boc-protected $^{\text{N}}$ -alkyl- N -(2-aminoethyl)glycine or $^{\text{N}}$ -acyl- N -(2-aminoethyl)glycine monomers (200 mg) at ice-cooled temperature. The reaction mixture was stirred for 1 h, concentrated, and the obtained product was dissolved in *sec*-butanol (10 mL) and heated at reflux at 110 °C under an argon atmosphere for 10–12 h. Reaction was monitored by TLC, and on completion of the reaction, the solvent was evaporated and the crude product was purified by silica gel column chromatography.

Yeast culture and growth assay

S. cerevisiae (strain BY 4741) was inoculated into YPD (1% yeast extract, 2% peptone, and 2% dextrose) medium and incubated for 8 h (30 °C, 250 rpm). From this primary inoculum, the secondary culture was inoculated and incubated as above until the culture absorbance (600 nm) reached 0.8. High-throughput growth curve analysis in the presence and absence of **4a** (50 μM) was performed using a Varioskan Flash apparatus from Thermo Scientific by recording the absorbance (600 nm) after every 20 min in a 384-well plate. The autophagy assay was performed in the yeast *P. pastoris*, in which degradation of cargo was followed over time upon induction of autophagy. The time taken for a 50% decrease in cargo activity was plotted for untreated cells and the compounds at 50 μM concentration. Triplicate values for the control were plotted and a difference of 3 standard deviation (SD) units between the test and control was considered as significant. For the fluorescence microscopy assay, *S. cerevisiae* cells were checked for selective degradation of peroxisomes through autophagy with or without compound **4a**. Microscopic images were obtained using a Zeiss confocal microscope.

GFP-Atg8 processing assay

S. cerevisiae strain containing the GFP-Atg8 (pRS 416 vector backbone) plasmid was grown in synthetic complete medium lacking uracil (SC-URA) under appropriate conditions (30 °C, 250 rpm). From this, a secondary culture was inoculated at $A_{600}=0.2$ and grown as above until A_{600} reached 0.65. The cultures were transferred to SD-N (nitrogen starvation) medium at $A_{600}=3$, separately with and without **4a** (50 μM), and at time points (0, 1, 2, 4, and 6 h) were collected at A_{600} equivalent of 3. Proteins were precipitated using trichloroacetic acid and samples were resolved by sodium dodecyl sulfate–polyacrylamide gel electrophoresis (10%) followed

by immunoblotting and probing with anti-GFP primary antibody (1:3000) and anti-mouse secondary antibody (1:10000).

Acknowledgements

We thank Prof. C. N. R. Rao FRS for constant support, JNCASR, the Department of Biotechnology (DBT)–Innovative Young Biotechnology Award (IYBA, grant BT/03/IYBA/2010), the Department of Science and Technology (DST), and Wellcome-DBT India Alliance for financial support, and Arkamita for modeling studies.

Keywords: autophagy • cyclization • hydrogen bonds • peptoids • synthetic methods

- [1] a) C. J. White, A. K. Yudin, *Nat. Chem.* **2011**, *3*, 509–524; b) A. Thakkar, T. B. Trinh, D. Pei, *ACS Comb. Sci.* **2013**, *15*, 120–129; c) S. A. Fowler, D. M. Stacy, H. E. Blackwell, *Org. Lett.* **2008**, *10*, 2329–2332.
- [2] a) Y. D. Wu, S. Gellman, *Acc. Chem. Res.* **2008**, *41*, 1231–1242; b) R. M. J. Liskamp, D. T. S. Rijkers, J. A. W. Kruijtzter, J. Kemmink, *ChemBioChem* **2011**, *12*, 1626–1653.
- [3] a) S. A. Fowler, H. E. Blackwell, *Org. Biomol. Chem.* **2009**, *7*, 1508–1524; b) N. C. Tan, P. Yu, Y. U. Kwon, T. Kodadek, *Bioorg. Med. Chem.* **2008**, *16*, 5853–586; c) C. A. Olsen, *ChemBioChem* **2010**, *11*, 134–160; d) E. Nnanabu, K. Burgess, *Org. Lett.* **2006**, *8*, 1259–1262.
- [4] O. Ovadia, Y. Linde, C. Haskell-Luevano, M. L. Dirain, T. Sheynis, R. Jelinek, C. Gilon, A. Hoffman, *Bioorg. Med. Chem.* **2010**, *18*, 580–589.
- [5] a) S. B. Y. Shin, B. Yoo, L. Todaro, J. K. Kirshenbaum, *J. Am. Chem. Soc.* **2007**, *129*, 3218–3225; b) O. Roy, S. Faure, V. Thery, C. Didierjean, C. Taillefumier, *Org. Lett.* **2008**, *10*, 921–924.
- [6] a) T. Godballe, L. L. Nilsson, P. D. Petersen, H. Jenssen, *Chem. Biol. Drug Des.* **2011**, *77*, 107–116; < *lit* b > J. E. Murphy, T. Uno, J. D. Hamer, F. E. Cohen, V. Dwarki, R. Zuckermann, *Proc. Natl. Acad. Sci. USA* **1998**, *95*, 1517–1522; c) L. Zhang, J. Yu, H. Pan, P. Hu, Y. Hao, W. Cai, H. Zhu, A. D. Yu, X. Xie, D. Ma, J. Yuan, *Proc. Natl. Acad. Sci. USA* **2007**, *104*, 19023–19028.
- [7] T. Fleming, T. Noda, T. Yoshimori, D. C. Rubinsztein, *Nat. Chem. Biol.* **2011**, *7*, 9–17.
- [8] M. Egholm, P. E. Nielsen, O. Buchardt, R. H. Berg, *J. Am. Chem. Soc.* **1992**, *114*, 9677–9678.
- [9] N. Kaur, B. Zhou, F. Breitbeil, K. Hardy, K. S. Kraft, I. Trantcheva, O. Phanstiel Iv, *Mol. Pharm.* **2008**, *5*, 294–315.
- [10] F. Cordier, S. Grzesiek, *J. Mol. Biol.* **2002**, *317*, 739–751.
- [11] T. R. White, C. M. Renzelman, A. C. Rand, T. Rezai, C. M. McEwen, V. M. Gelev, R. A. Turner, R. G. Linington, S. S. F. Leung, A. S. Kalgutkar, J. N. Bauman, Y. Z. Zhang, S. Liras, D. A. Price, A. M. Mathiowetz, M. P. Jacobson, R. S. Lokey, *Nat. Chem. Biol.* **2011**, *7*, 810–817.
- [12] T. Cierpicki, J. Otlewski, *J. Biomol. NMR* **2001**, *21*, 249–261.
- [13] N. Maulucci, I. Izzo, G. Bifulco, A. Aliberti, C. De Cola, D. Comegna, C. Gaeta, A. Napolitano, C. Pizza, C. Tedesco, D. Flot, F. De Riccardis, *Chem. Commun.* **2008**, 3927–3929.
- [14] J. E. Baldwin, *J. Chem. Soc. Chem. Commun.* **1976**, 734–736.
- [15] a) E. Santis, T. Hjelmggaard, S. Faure, O. Roy, C. Didierjean, B. Alexander, G. Siligardi, R. Hussain, T. Javorfi, A. Edwards, C. Taillefumier, *Amino Acids* **2011**, *41*, 663–672; b) Y.-U. Kwon, T. Kodadek, *J. Am. Chem. Soc.* **2007**, *129*, 1508–1509.

Received: October 7, 2013

Published online on December 11, 2013